12. Wakimoto, B. T. Beyond the nucleosome: epigenetic aspects of position-effect variegation in Drosophila. *Cell* **93**, 321–324 (1998).

13. Boivin, A. & Dura, J. M. In vivo chromatin accessibility correlates with gene silencing in Drosophila. *Genetics* **150**, 1539–1549 (1998).

14. Gottschling, D. E. Telomere-proximal DNA in Saccharomyces cerevisiae is refractory to methyl-transferase activity in vivo. *Proc. Natl Acad. Sci. USA* **89**, 4062–4065 (1992).

15. Braunstein, M., Sobel, R. E., Allis, C. D., Turner, B. M. & Broach, J. R. Efficient transcriptional silencing in Saccharomyces cerevisiae requires a heterochromatin histone acetylation pattern. *Mol. Cell Biol.* **16**, 4349–4356 (1996).

16. Turner, B. M., Birley, A. J. & Lavender, J. Histone H4 isoforms acetylated at specific lysine residues define individual chromosomes and chromatin domains in Drosophila polytene nuclei. *Cell* **69**, 375–384 (1992).

17. Dorer, D. R. & Henikoff, S. Expansions of transgene repeats cause heterochromatin formation and gene silencing in Drosophila. *Cell* **77**, 993–1002 (1994).

18. Devlin, R. H., Bingham, B. & Wakimoto, B. T. The organization and expression of the light gene, a heterochromatic gene of Drosophila melanogaster. *Genetics* **125**, 129–140 (1990).

19. Dorsett, D. Distant liaisons: long-range enhancer-promoter interactions in Drosophila. *Curr. Opin. Genet. Dev.* **9**, 505–514 (1999).

20. Durfee, T. *et al.* The retinoblastoma protein associates with the protein phosphatase type 1 catalytic subunit. *Genes Dev.* **7**, 555–569 (1993).

21. Sandell, L. L., Gottschling, D. E. & Zakian, V. A. Transcription of a yeast telomere alleviates telomere position effect without affecting chromosome stability. *Proc. Natl Acad. Sci. USA* **91**, 12061–12065 (1994).

22. Bourns, B. D., Alexander, M. K., Smith, A. M. & Zakian, V. A. Sir proteins, Rif proteins, and Cdc13p bind Saccharomyces telomeres in vivo. *Mol. Cell Biol.* **18**, 5600–5608 (1998).

23. Alexander, C., Grueneberg, D. A. & Gilman, M. Z. Studying heterologous transcription factors in yeast. *Methods Companion Methods Enzymol.* **5**, 147–155 (1993).

24. Braunstein, M., Rose, A. B., Holmes, S. G., Allis, C. D. & Broach, J. R. Transcriptional silencing in yeast is associated with reduced nucleosome acetylation. *Genes Dev.* **7**, 592–604 (1993).

Direct observation of DNA rotation during transcription by *Escherichia coli* RNA polymerase

Yoshie Harada[*†‡], **Osamu Ohara**[§], **Akira Takatsuki**[*], **Hiroyasu Itoh**[†∥], **Nobuo Shimamoto**[¶] **& Kazuhiko Kinosita Jr**[*†]

* *Department of Physics, Faculty of Science and Technology, Keio University, Hiyoshi 3-14-1, Kohoku-ku, Yokohama 223-8522, Japan*
† *CREST (Core Research for Evolutional Science and Technology) "Genetic Programming" Team 13, Nogawa 907, Miyamae-ku, Kawasaki 216-0001, Japan*
§ *Kazusa DNA Research Institute, Yana 1532-3, Kisarazu 292-0812, Japan*
∥ *Tsukuba Research Laboratory, Hamamatsu Photonics KK, Tokodai, Tsukuba 300-2635, Japan*
¶ *Structural Biology Center, National Institute of Genetics, Mishima 411-8540, Japan*

Helical filaments driven by linear molecular motors are anticipated to rotate around their axis, but rotation consistent with the helical pitch has not been observed. 14S dynein[1] **and non-claret disjunctional protein (ncd)**[2] **rotated a microtubule more efficiently than expected for its helical pitch, and myosin rotated an actin filament only poorly**[3]**. For DNA-based motors such as RNA polymerase, transcription-induced supercoiling of DNA**[4] **supports the general picture of tracking along the DNA helix**[5]**. Here we report direct and real-time optical microscopy measurements of rotation rate that are consistent with high-fidelity tracking. Single RNA polymerase molecules attached to a glass surface rotated DNA for >100 revolutions around the right-handed screw axis of the double helix with a rotary torque of >5 pN nm. This real-time observation of rotation opens the possibility of resolving individual transcription steps.**

Linear movement of a single molecule of RNA polymerase relative to DNA has been observed directly, during transcription[6–9] and during a one-dimensional diffusional search for a promoter[8,10,11]. To observe relative rotation between RNA polymerase and DNA, we employed an optical microscopy technique based on the tethered-particle method[6] (Fig. 1a). A DNA template, 4,971 base pairs (1.7 μm) long and containing one strong promoter (T7A1), was constructed (Fig. 1b). Transcription was initiated in a bulk solution in the absence of UTP, such that the polymerase stalled at the adenine at the +20 position (A20), before the thymine at +21 position[12]. The stalled polymerase was attached to a glass surface (Fig. 1a), and a magnetic bead of diameter 850 nm coated with streptavidin was attached to the downstream end of the DNA where nine nucleotide residues were biotinylated. Then, all four nucleoside triphosphates (NTPs) were added to allow further transcription. In a similar system with a non-magnetic bead, Schafer et al.[6] observed highly 'processive' (moving over a long distance without detachment) threading of DNA through RNA polymerase,
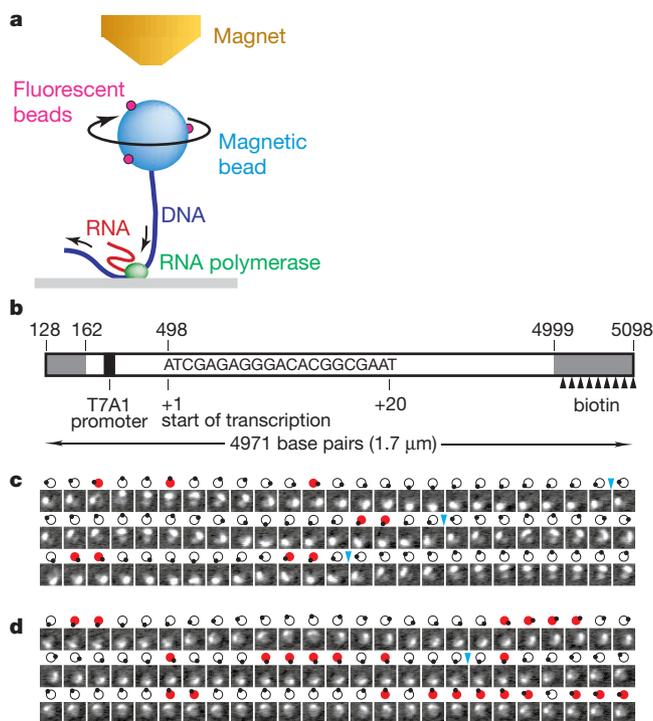

Figure 1 Observation of DNA rotation by RNA polymerase. **a**, Observation system (not to scale). The magnetic bead was pulled upwards by a disk-shaped neodymium magnet, to which a conical iron piece was attached to enhance the magnetic force. Magnetization was vertical and did not prevent bead rotation. Daughter fluorescent beads served as markers of rotation. **b**, The DNA template. Numbers above are from the T7 D111 sequence. Rotation assay started from position +20. The magnetic bead was attached to the nine biotins. Shaded ends denote primers for the polymerase chain reaction. **c**, **d**, Snapshots of rotating beads at 133-ms intervals at NTP concentrations of 50 μM (**c**) and 2.5 μM (**d**). Grey part at the centre, a magnetic bead visualized with transmitted light; moving white spot, a daughter fluorescent bead or probably its aggregates. Diagrams show their relative positions. Blue arrowheads indicate completion of a turn. Red diagrams show moments of anticlockwise rotation due to torsional brownian fluctuations of DNA; these were less noticeable at high [NTP], presumably because supercoiling had reduced the effective tether length. Image size, 2.4 × 2.4 μm².

113

visualized as progressive reduction in the range of the brownian motion of the end bead. We also confirmed this. The high processivity, however, does not necessarily imply precise helical tracking. RNA polymerase might occasionally allow DNA to rotate freely within the active site to relieve torsional stress. Or, the polymerase might allow transient, straight backward slippage of DNA without rotation, while imposing helical rotation for forward movement. This would lead to overwinding. For forward movement, RNA polymerase might bring in DNA several base pairs at a time, in which case tracking of the double helix is not required.

We thus attempted to observe rotation directly by decorating the end bead with smaller fluorescent beads. We pulled the magnetic bead upward at ~0.1 pN with a magnet for two reasons: to confine the rotation in a horizontal plane, and in the hope of restraining the DNA from supercoiling, which would interfere with torque transmission to the end bead. Up to a few per cent of beads in an observation chamber rotated continuously (Fig. 1c, d), invariably clockwise when viewed from top in Fig. 1a. Threading a right-handed double helix of DNA through RNA polymerase will, in a simple mechanism, produce clockwise rotation. Not all beads rotated, some being stuck on the glass surface; others fluctuated in both directions, presumably being attached to nicked DNA or tethered to an inactive polymerase. Below we report only on those beads that made at least five revolutions in one direction. When NTPs were absent, unidirectional rotation was not observed.

Time courses of rotation of individual beads are shown in Fig. 2. Most curves do not start at time zero, because we had to search over several fields of view before finding a continuously rotating bead. The curves are also shifted upwards to give the impression that all beads started rotating at time zero. In fact we could confirm this only for three cases. Generally the rotation was slower at lower NTP concentration, [NTP], although variations among beads were large. Extremely slow beads, among those examined under the same [NTP], often carried large aggregates of fluorescent beads. Rotation rate also varied with time. Thin parts of the curves in Fig. 2 indicate
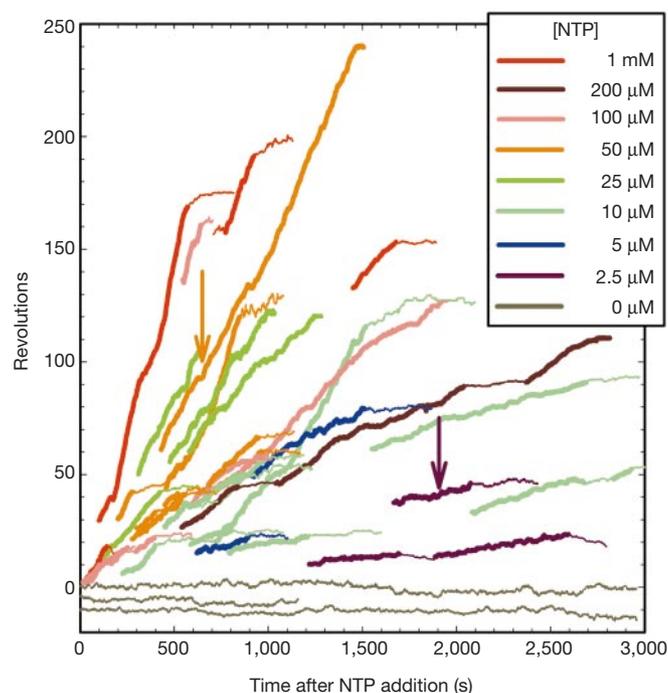
pauses in the bead rotation; we define a pause as a time interval longer than 50 s during which a bead fluctuated no more than ±2 revolutions (this was less well defined at low [NTP]). Observation was terminated after a pause, or after complete immobilization for >30 s, or when the bead tore off and floated into solution. For our DNA template with the full transcript length of ~4,500 bases, the expected number of revolutions is 4,500/10.4 (base pairs per turn of DNA[13]); that is, ~ 430. At least ~180 consecutive revolutions have been observed (an orange curve in Fig. 2), suggesting that thousands of base pairs can be transcribed without extensive rotational slippage.

To compare with the rate of rotation, we measured the rate of RNA elongation in solution, and on individual molecules of RNA polymerase on the glass surface[6] (see Supplementary Information). As summarized in Fig. 3, the two methods gave consistent results (dark versus light green symbols), indicating that surface attachment did not alter the elongation kinetics. The elongation rate divided by 10.4 will be the rotation rate if the polymerase faithfully tracks the DNA helix. Indeed, this seemed to be the case at [NTP] below ~20 μM, as seen in red circles in Fig. 3 (also see legend for the purple curve). Although the scatter in rotation data is large, we believe that data showing faster (and longer) rotation are more reliable, because anything that attaches or touches the bead impedes rotation (aggregates of fluorescent beads, DNA, and so on). These data support high-fidelity tracking, but we cannot dismiss the possibility of underwinding by a factor of up to ~2. Extensive overwinding is unlikely.

The apparent saturation of rotation rate in Fig. 3 is explained if the maximal torque of RNA polymerase, Γ_{max}, is already reached at the observed maximal rotation rate of ~0.2 revolutions per second (r.p.s.). To rotate a bead of diameter $D = 850$ nm in bulk water at this speed, a torque $\Gamma = 2\pi[0.2 \text{ r.p.s.}]\xi \approx 2.4$ pN nm is required, where $\xi = \pi\eta D^3$ is the rotational frictional drag coefficient and η ($= 10^{-9}$ pN nm^{-2} s) is the viscosity of water. The drag is higher

Figure 2 Time courses of bead rotation at various [NTP]. Rotation angles (clockwise positive) were estimated from images as in Fig. 1c, d by centroid analysis[17]. Thin lines indicate portions that were excluded in the estimation of rotation rates in Fig. 3. Arrows show the portions shown in Fig. 1c, d.
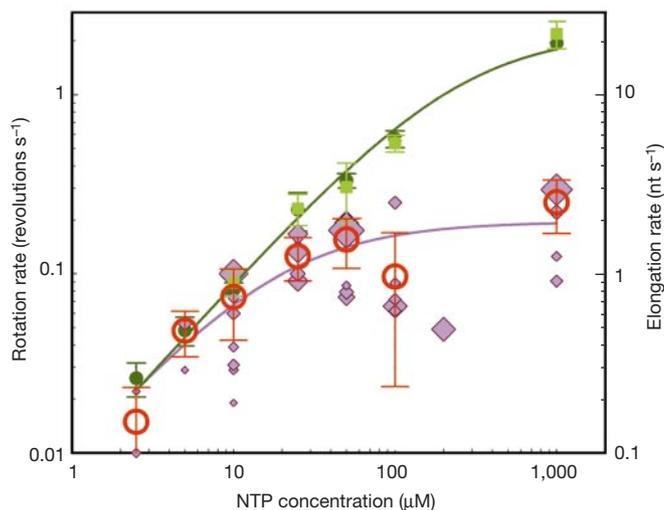

Figure 3 Comparison of rotation and transcription rates. Purple diamonds, rotation rates for individual beads, estimated as the total number of revolutions, N, in the thick portion of a curve in Fig. 2 divided by time; symbol size $\propto N^{1/2}$. Red circles, rotation rates at indicated [NTP] averaged with weights $\propto N$; error bars, root mean square of weighted residuals. Dark green circles, elongation rates in solution; light green squares, elongation rates for individual RNA polymerase molecules on the glass surface (see Supplementary Information). Dark green curve, fit with $V = V_{max}[\text{NTP}]/([\text{NTP}] + K_m)$ where $V_{max} = 22$ nucleotides s^{-1} and $K_m = 250$ μM. Purple curve, fit to purple diamonds with rotation rate r given by[17] $1/r = n/V + T_{rot}$; n/V is the time for elongation reaction where n nucleotides are added per revolution; T_{rot} is the time required to rotate the bead against friction; $n = 8.7 \pm 3.7$ nucleotides per revolution ($n = 10.4$ for precise helical tracking) and $T_{rot}^{-1} = 0.21 \pm 0.8$ r.p.s.

near the glass surface[14]. Pulled at ~0.1 pN by the magnet, the bead centre will be ~1.1 μm from the surface at the initial DNA length of ~1.5 μm (ref. 15). The effective ξ at this height is ~130% of the bulk value, and approaches 300% as the bead comes down towards the surface[14]. DNA itself must also rotate, with a similar magnitude of ξ. Altogether, the required torque will be >5 pN nm. Flexible DNA cannot sustain this much torque and collapses by supercoiling, which is expected to occur at the critical torque $\Gamma_c \approx 6$ pN nm under ~0.1 pN of tension[15]. At high [NTP], beads often rotated steadily without lateral fluctuations, suggesting that extensive supercoiling had made the effective tether length approximately equal to zero. The beads may then touch the surface, further increasing the effective ξ. Presumably, balance between this high drag and Γ_{max} is reached at ~0.2 r.p.s. ($= \Gamma_{max}/2\pi\xi = T_{rot}^{-1}$ in Fig. 3 legend), resulting in saturation. Γ_{max} must be >5 pN nm, but is unlikely to exceed the 40 pN nm which F_1-ATPase produces by converting available energy almost entirely to rotation[16,17]. An alternative explanation for the slow rotation at high [NTP] might be extensive rotary slippage in RNA polymerase at [NTP] > 20 μM. However, simple slippage is unlikely to result in the saturation behaviour, and the transcription obeyed simple Michaelis–Menten kinetics—indicative of an [NTP]-independent mechanism.

In summary, our results indicate that RNA polymerase rotates DNA by tracking its right-handed helix, that the polymerase does so over thousands of base pairs, and that the polymerase can produce >5 pN nm of torque. Whether RNA polymerase rotates around DNA or vice versa is an issue *in vivo*[5], but our experiment with fixed RNA polymerase cannot answer this problem. Some uncertainty remains in the degree of tracking fidelity, but several beads made many revolutions at the rate commensurate with precise helical tracking. Although the mechanism of tracking is yet unknown, genuine rotary motors may also employ tracking as the rotary mechanism. In the bacterial flagellar motor[18,19], the rotor consists of circularly arranged identical subunits. Driving units are also circularly arranged, but one unit suffices to produce efficient rotation[19]. A single unit may thus track along the rotor subunits thereby causing rotation. In the F_1-ATPase in which an asymmetric rotor rotates in 120° steps[17], the tracking mechanism is unlikely.

We expect that the RNA polymerase rotation reported here could provide a means of resolving individual steps of transcription. Transcription of one base will produce a linear translocation of 0.34 nm (ref. 13), which is extremely difficult to resolve. However, accompanying rotation is as much as 35°, and should in principle be detectable. The main problem is torsional brownian motion of DNA, which has to be averaged out. A tag much smaller than the 850-nm bead (and shorter DNA) is needed for averaging within a reasonable time. Determination of the orientation of a tiny tag is feasible, even of a single fluorophore[3,20]. □

Methods

Materials

Escherichia coli RNA polymerase holoenzyme was purified[21] and supplemented with excess σ-subunit. The DNA template for transcription was prepared from T7 D111 DNA[22], by polymerase chain reaction with an upstream primer for segment 128–162 (in the T7 coordinate) and downstream primer for 4999–5098 (Fig. 1b). The downstream primer had been biotinylated at 9 sites at ~10-base intervals. Before use, the template was treated with T4 DNA ligase at 0.1 mM ATP for 30 min at room temperature to remove nicks. Stalled transcription complex[12] was prepared by incubating 0.3 μM RNA polymerase and 0.3 nM DNA in buffer A (20 mM TrisCl pH 8.0, 20 mM NaCl, 14 mM MgCl₂, 0.1 mM EDTA, 14 mM 2-mercaptoethanol, 1.5% (w/v) glycerol, 20 μg ml⁻¹ acetylated BSA, 250 μM ApU dinucleotide) containing 100 μM each of ATP, GTP and CTP for 3 min at 30 °C.

Fluorescent, carboxylated microbeads (20 nm, excitation 580 nm, emission 605 nm, Molecular Probes) were amino-derivatized with ethylene diamine in the presence of 1-ethyl-3-(3-dimethylaminopropyl)carbodiimide (EDC). The microbeads and Biotin-X cadaverine (Molecular Probes) were conjugated to 850-nm carboxylated magnetic beads (Seradyn) with EDC, and streptavidin was bound to the biotinylated magnetic beads[11].

Transcription on the glass surface

A flow chamber[17] was made of two coverslips, which had been sonicated in water, stored in methanol, and dried by setting fire to the methanol. 5 μl of stalled complex in buffer A was mixed with 50 μl of buffer B (20 mM Tris-acetate pH 8.0, 130 mM NaCl, 4 mM MgCl₂, 0.1 mM EDTA, 0.1 mM DTT, 20 μg ml⁻¹ acetylated BSA and 80 μg ml⁻¹ heparin), infused into the flow chamber, and incubated for 5 min. Further treatments were infusion of 2 mg ml⁻¹ α-casein in buffer B for 2 min; washing with buffer B; infusion of beads in buffer C (buffer B minus BSA and heparin, plus 1 mg ml⁻¹ α-casein) for 15 min; washing with buffer B plus 1 mM biotin; then washing with buffer B. Transcription was started by infusing NTPs and 0.5% (v/v) 2-mercaptoethanol in buffer B.

Microscopy

Samples were observed at 23 ± 2 °C on an Olympus IX70 inverted microscope with a 100× oil-immersion objective. Magnetic beads were illuminated with a halogen lamp obliquely from above through a ring-shaped optical-fibre assembly. Fluorescent daughter beads were imaged with standard epi-fluorescence optics. Superimposed bright-field and fluorescence images were projected on a silicon-intensified target camera (C2400-08 Hamamatsu Photonics) and recorded on a video tape. A conical magnet was placed above the sample to pull the beads (Fig. 1a). Vertical pulling force was calibrated by tethering the magnetic beads with 16-μm-long λ-phage DNA and measuring the amplitude of brownian motion[15]. The force varied among beads and was 0.05–0.2 pN.

1. Vale, R. D. & Toyoshima, Y. Y. Rotation and translocation of microtubules in vitro induced by dyneins from *Tetrahymena* cilia. *Cell* **52,** 459–469 (1988).
2. Walker, R. A., Salmon, E. D. & Endow, S. A. The *Drosophila claret* segregation protein is a minus-end directed motor molecule. *Nature* **347,** 780–782 (1990).
3. Sase, I., Miyata, H., Ishiwata, S. & Kinosita, K. Jr Axial rotation of sliding actin filaments revealed by single-fluorophore imaging. *Proc. Natl Acad. Sci. USA* **94,** 5646–5650 (1997).
4. Wang, J. C. & Lynch, A. S. Transcription and DNA supercoiling. *Curr. Opin. Genet. Dev.* **3,** 764–768 (1993).
5. Cook, P. R. The organization of replication and transcription. *Science* **284,** 1790–1795 (1999).
6. Schafer, D. A., Gelles, J., Sheetz, M. P. & Landick, R. Transcription by single molecules of RNA polymerase observed by light microscopy. *Nature* **352,** 444–448 (1991).
7. Wang, M. D. *et al.* Force and velocity measured for single molecules of RNA polymerase. *Science* **282,** 902–907 (1999).
8. Guthold, M. *et al.* Direct observation of one-dimensional diffusion and transcription by *Escherichia coli* RNA polymerase. *Biophys. J.* **77,** 2284–2294 (1999).
9. Davenport, R. J., Wuite, G. J. L., Landick, R. & Bustamante, C. Single-molecule study of transcriptional pausing and arrest by *E. coli* RNA polymerase. *Science* **287,** 2497–2500 (2000).
10. Kabata, H. *et al.* Visualization of single molecules of RNA polymerase sliding along DNA. *Science* **262,** 1561–1563 (1993).
11. Harada, Y. *et al.* Single molecule imaging of RNA polymerase-DNA interactions in real time. *Biophys. J.* **76,** 709–715 (1999).
12. Levin, J. R., Krummel, B. & Chamberlin, M. J. Isolation and properties of transcribing ternary complexes of *Escherichia coli* RNA polymerase positioned at single template base. *J. Mol. Biol.* **196,** 85–100 (1987).
13. Stryer, L. *Biochemistry* 4th edn (Freeman, New York, 1995).
14. Svoboda, K. & Block, S. M. Biological applications of optical tweezers. *Annu. Rev. Biophys. Biomol. Struct.* **23,** 247–285 (1994).
15. Strick, T., Allemand, J.-F., Bensimon, D., Lavery, R. & Croquette, V. Phase coexistence in a single DNA molecule. *Physica A* **263,** 392–405 (1999).
16. Noji, H., Yasuda, R., Yoshida, M. & Kinosita, K. Jr Direct observation of the rotation of F_1-ATPase. *Nature* **386,** 299–302 (1997).
17. Yasuda, R., Noji, H., Kinosita, K. Jr & Yoshida, M. F_1-ATPase is a highly efficient molecular motor that rotates with discrete 120° steps. *Cell* **93,** 1117–1124 (1998).
18. DeRosier, D. J. The turn of the screw: the bacterial flagellar motor. *Cell* **93,** 17–20 (1998).
19. Ryu, W. S., Berry, R. M. & Berg, H. C. Torque-generating units of the flagellar motor of *Escherichia coli* have a high duty ratio. *Nature* **403,** 444–447 (2000).
20. Adachi, K. *et al.* Stepping rotation of F_1-ATPase visualized through angle-resolved single-fluorophore imaging. *Proc. Natl Acad. Sci. USA* **97,** 7243–7247 (2000).
21. Kubori, T. & Shimamoto, N. A branched pathway in the early stage of transcription by *Escherichia coli* RNA polymerase. *J. Mol. Biol.* **256,** 449–457 (1996).
22. Studier, F. W. Gene 0·3 of bacteriophage T7 acts to overcome the DNA restriction system of the host. *J. Mol. Biol.* **94,** 283–295 (1975).